



HAL
open science

In-situ forming plga implants for intraocular dexamethasone delivery

C. Bode, Heiko Kranz, Florence Siepmann, Juergen Siepmann

► To cite this version:

C. Bode, Heiko Kranz, Florence Siepmann, Juergen Siepmann. In-situ forming plga implants for intraocular dexamethasone delivery. *International Journal of Pharmaceutics*, 2018, *International Journal of Pharmaceutics*, 548, pp.337-348. 10.1016/j.ijpharm.2018.07.013 . hal-04467257

HAL Id: hal-04467257

<https://hal.univ-lille.fr/hal-04467257>

Submitted on 29 Apr 2024

HAL is a multi-disciplinary open access archive for the deposit and dissemination of scientific research documents, whether they are published or not. The documents may come from teaching and research institutions in France or abroad, or from public or private research centers.

L'archive ouverte pluridisciplinaire **HAL**, est destinée au dépôt et à la diffusion de documents scientifiques de niveau recherche, publiés ou non, émanant des établissements d'enseignement et de recherche français ou étrangers, des laboratoires publics ou privés.

1
2
3
4
5
6
7
8
9
10
11
12
13
14
15
16
17
18
19
20
21
22
23
24
25

Research article

***In-situ* forming PLGA implants for intraocular dexamethasone delivery**

C. Bode,¹ H. Kranz,² F. Siepmann,¹ J. Siepmann,^{1,*}

¹*Univ. Lille, Inserm, CHU Lille, U1008, 59000 Lille, France*

²*Bayer AG, Muellerstraße 178, 13353 Berlin, Germany*

*correspondence:

Professor Juergen Siepmann, Ph.D.

Univ. Lille, College of Pharmacy,

INSERM U1008 Controlled Drug Delivery Systems and Biomaterials

3, rue du Professeur Laguesse

59006 Lille, France

Phone: +33-3-20964708

juergen.siepmann@univ-lille2.fr

26 **Abstract**

27 Different types of *in-situ* forming implants based on poly(lactic-co-glycolic acid) (PLGA) and
28 N-methyl-pyrrolidone (NMP) were prepared for controlled ocular delivery of dexamethasone.
29 The impact of the volume of the release medium, initial drug content, polymer molecular weight
30 and PLGA concentration on the resulting drug release kinetics were studied and explained
31 based on a thorough physico-chemical characterization of the systems. This included for
32 instance the monitoring of dynamic changes in the implants' wet and dry mass, morphology,
33 PLGA polymer molecular weight, pH of the surrounding bulk fluid and water/NMP contents
34 upon exposure to phosphate buffer pH 7.4. Importantly, the systems can be expected to be rather
35 robust with respect to variations in the vitreous humor volumes encountered *in vivo*.
36 Interestingly, limited drug solubility effects *within* the implants as well as in the surrounding
37 aqueous medium play an important role for the control of drug release at a drug loading of only
38 7.5 %. Furthermore, the polymer molecular weight and PLGA concentration in the liquid
39 formulations are decisive for *how* the polymer precipitates during solvent exchange and for the
40 swelling behavior of the systems. These features determine the resulting inner system structure
41 and the conditions for mass transport. Consequently, they affect the degradation and drug
42 release of the *in-situ* formed implants.

43

44 *Key words:* PLGA; *in-situ* forming implant; dexamethasone; autocatalysis; swelling

45 1. Introduction

46 Age-related macular degeneration (AMD) and diabetic retinopathy are two of the leading
47 causes for irreversible blindness and vision impairment (Hughes et al., 2005; Edelhauser et al.,
48 2010). Late AMD exists in two forms: the atrophic (or “dry”) AMD and the neovascular (or
49 “wet”) AMD. Yet, up to now, wet AMD is the only treatable form. It is triggered by vascular
50 endothelial growth factor (VEGF), causing the blood vessels in the retina to grow erratically,
51 eventually breaking through the Bruch’s membrane (the innermost layer of the choroid). This
52 leads to blood and protein leakage in the macula, resulting in a blurry vision or sudden vision
53 loss (Chiou, 2011; Bonilha et al., 2013). In the case of diabetic retinopathy, microvascular
54 complications are the result of poorly adjusted diabetes. Sustained hyperglycaemia ultimately
55 causes microaneurysms and a breakdown of endothelial tight junctions in the blood-retinal
56 barrier (BRB), allowing proteins to leak into the vitreous. At later stages, choroidal
57 neovascularization of the retina occurs (Kowluru and Mishra, 2015; Wan et al., 2015; Zaki et
58 al., 2016). Both diseases (wet AMD and diabetic retinopathy) are commonly treated by
59 intravitreal injections of anti-VEGF agents and corticosteroids. Anti-VEGF agents inhibit the
60 growth of the blood vessels, while corticosteroids reduce inflammation by minimizing the
61 expression of inflammatory cytokines and of VEGF. Hence, the choroidal neovascularization
62 is stabilized, decreasing the breakdown rate of the blood-retinal barrier (Kurz et al., 2008;
63 Wykoff et al., 2015; Rodríguez Villanueva et al., 2017).

64 For an effective treatment, the drugs have to reach the retina in the back of the eye.
65 However, the anatomy and physiology of the eye hamper this: For instance, when using eye
66 drops, less than 5% of the administered drug is generally absorbed through the cornea to reach
67 the anterior chamber (Urtti, 2006). This is due to the low permeability of the cornea (with its
68 different layers and polarities), dilution with tear fluid, rapid lacrimal drainage and other factors.
69 Most importantly, only a very small fraction of the drug is finally found inside the vitreous: the

70 site of action (approximately 0.001 – 0.0004 % of the administered drug) (Urtti, 2006; Wilson
71 et al., 2011; Kaur and Kakkar, 2014). It has to be pointed out that systemic drug administration
72 also encounters a crucial hurdle: The blood-retinal barrier, preventing most drugs from reaching
73 the vitreous. The attempt to overcome this hurdle with very high systemically administered
74 drug amounts to achieve therapeutic levels in the eye is limited by severe side effects
75 (Edelhauser et al., 2010; Kaur and Kakkar, 2014).

76 For these reasons intravitreal drug injections are currently considered as the most
77 appropriate way to assure that the drug reaches its site of action. However, every injection bears
78 a risk of infections and other serious side effects, like retinal detachment, retinal haemorrhage,
79 endophthalmitis, increased intraocular pressure, cataract or vitreous haemorrhage (Edelhauser
80 et al., 2010; Giudice and Galan, 2012; Ying et al., 2013; Kaur and Kakkar, 2014; Bisht et al.,
81 2017). Apart from these risks, the discomfort of receiving a needle in the eye leads to limited
82 compliance (Droege et al., 2013; Ghazala et al., 2013).

83 To assure treatment efficacy, therapeutic drug concentrations must be provided over
84 prolonged periods of time at the site of action. Since dexamethasone has a half-life of
85 approximately 5.5 h in the vitreous, frequent injections are, thus, necessary to remain within
86 the therapeutic range (Chan et al., 2011). Local controlled drug delivery systems can help
87 overcoming all these hurdles: The risk of side effects can be reduced, patient compliance
88 improved and the therapeutic efficacy increased. Nowadays, non-biodegradable implants are
89 approved by the FDA for intraocular administration, releasing dexamethasone over prolonged
90 periods of time [e.g., Retisert (retisert.com), Iluvien (iluvien.com)]. However, these implants
91 have to be removed surgically upon drug exhaust, which is associated with similar risks as the
92 initial insertion, or remain in the vitreous where they accumulate over time (Yasin et al., 2014).
93 To avoid the second surgery for device removal, *biodegradable* implants offer an interesting
94 potential. For example, Allergan developed Ozurdex, a biodegradable implant containing 0.7

95 mg dexamethasone in a poly(lactic-co-glycolic acid) (PLGA) matrix, which is injected through
96 a 22G needle (Chan et al., 2011). But large needles can be problematic in practice. The injection
97 of a *liquid* solution, that precipitates *in-situ* in the eye and sustains drug release, could
98 effectively reduce the required needle size. Importantly, smaller needles are associated with
99 less pain experienced by the patients (Rodrigues et al., 2011).

100 Different types of *in-situ* forming implants have been described in the literature, for various
101 types of applications (Kranz and Bodmeier, 2007, 2008; Schoenhammer et al., 2009, 2010;
102 Kempe and Mäder, 2012; Parent et al., 2013, 2017). The transformation from the liquid state
103 (allowing for facilitated administration) to the solid state (allowing for controlled drug release
104 over prolonged periods of time) can be induced by different phenomena, such as solvent
105 exchange, changes in the pH or temperature, or *in-situ* cross-linking (Kempe and Mäder, 2012).
106 In the case of solvent exchange, generally a water-insoluble polymeric matrix former is
107 dissolved in a biocompatible, water-miscible organic solvent. The drug is dissolved and/or
108 dispersed in this polymer solution. Upon injection into aqueous body fluids, the organic solvent
109 diffuses into the surrounding environment (being miscible with water), while water diffuses
110 into the formulation. Since the polymer is water-insoluble, it precipitates and forms the solid
111 implant. The drug molecules or particles are trapped within the implant and slowly released
112 over time. Different formulation parameters can be used to alter implant formation and
113 performance. For instance, the addition of hydrophilic polymers [such as hydroxypropyl
114 methylcellulose (HPMC)] has been proposed to increase the bioadhesion of *in-situ* forming
115 implants releasing antimicrobial drugs in periodontal pockets for the treatment of periodontitis
116 (Do et al., 2014, 2015b, 2015a; Agossa et al., 2017). Poly(lactic-co-glycolic acid) (PLGA) is a
117 well-known biodegradable and biocompatible matrix former in parenteral controlled release
118 formulations (Kranz et al., 2000; Luan et al., 2006; Desai et al., 2008; Kempe et al., 2010;
119 Fredenberg et al., 2011; Ghalanbor et al., 2013; Schwendeman et al., 2014; Gasmi et al., 2015a,

120 2015b; Huang et al., 2015; Gasmi et al., 2016; Hirota et al., 2016; Hamoudi-Ben Yelles et al.,
121 2017). In the case of *in-situ* forming implants based on PLGA, often N-methyl-pyrrolidone
122 (NMP) is used as a water-miscible organic solvent, for example in the following commercially
123 available drug products: Atridox (for injection into periodontal pockets) (Thakur et al., 2014);
124 Eligard (for subcutaneous injection) (eligard.com); Nuflor (for intramuscular or subcutaneous
125 injection in beef) (merck-animal-health-usa.com/product/cattle/Nuflor-Injectable-Solution/1);
126 Doxirobe gel (for injection into periodontal pockets in dogs)
127 (zoetisus.com/products/dogs/doxirobe-gel.aspx). Furthermore, the group of AG Mikos (Ueda
128 et al., 2007) reported on NMP-based *in-situ* forming ocular drug delivery systems for
129 luocinolone acetonide, which are based on poly(propylene fumarate) as polymeric matrix
130 former. It has to be pointed out that the toxicity of NMP upon intraocular injection should be
131 investigated in the future.

132 The aim of this study was to prepare different types of *in-situ* forming implants based on
133 PLGA for intraocular dexamethasone delivery. The systems were thoroughly characterized
134 physico-chemically, including for instance dynamic changes in the wet mass, dry mass,
135 water/NMP content, morphology, polymer molecular weight, potential changes in the pH of the
136 release medium, and drug release kinetics.

137

138

139 **2. Materials and methods**

140

141 **2.1. Materials**

142 Poly(D,L-lactic-co-glycolic acid) (50:50, -COOH end groups; PLGA, Resomer RG 502 H
143 and Resomer RG 504 H; Evonik, Darmstadt, Germany); dexamethasone (Discovery Fine
144 Chemicals, Dorset, UK); N-methyl-pyrrolidone, acetonitrile and tetrahydrofuran (Fisher
145 Scientific, Illkirch, France); ethanol 96% (VWR, Fontenay-sous-Bois, France).

146

147 **2.2. Preparation of the liquid formulations**

148 Appropriate amounts of PLGA and dexamethasone were dissolved in NMP in glass vials
149 under stirring at 500 rpm (Multipoint Stirrer, Thermo Scientific, Loughborough, UK) at room
150 temperature for 60 min. Afterwards, the vials were kept without stirring for 1 h at room
151 temperature in order to remove air bubbles. The formulations were stored at 2-8 °C, and allowed
152 to reach room temperature prior to use.

153

154 **2.3. *In-situ* formation of implants**

155 Eppendorf vials were filled with 2.25 or 4.5 mL phosphate buffer pH 7.4 (USP 40) and kept
156 at 37 °C overnight. One hundred µl of the liquid PLGA/dexamethasone/NMP formulations
157 (prepared as described in *section 2.2.*) were injected into the vials using a syringe pump
158 (2 mL/min; PHD 2000; Harvard Apparatus, Holliston, USA). Solvent exchange initiated
159 polymer precipitation and *in-situ* implant formation. The Eppendorf vials were placed into a
160 horizontal shaker (80 rpm, 37 °C; GFL 3033, Gesellschaft fuer Labortechnik, Burgwedel,
161 Germany).

162

163 **2.4. Characterization of *in-situ* formed implants**

164 In vitro drug release: At determined time points, the phosphate buffer pH 7.4 was
165 completely renewed. The amount of dexamethasone in the withdrawn bulk fluid was
166 determined by HPLC-UV analysis, using a Thermo Fisher Scientific Ultimate 3000 Series
167 HPLC, equipped with a LPG 3400 SD/RS pump, an auto sampler (WPS-3000 SL) and a UV-
168 Vis detector (VWD-3400RS) (Thermo Fisher Scientific, Waltham, USA). Samples were
169 centrifuged for 2.5 min at 10,000 rpm (Centrifuge Universal 320; Hettich, Tuttlingen,
170 Germany), and filtered with a 0.45 µm PVDF syringe filter (Millex-HV, Merck Millipore,

171 Tullagreen, Ireland). Fifty μL samples were injected into an A C18 RP column (Gemini 3 μm
 172 C18 110 Å, 100 mm x 4.6 mm; Phenomenex, Le Pecq, France). The mobile phase consisted of
 173 acetonitrile and water (33:67 v/v), the flow rate was 1.5 mL/min. Dexamethasone had a
 174 retention time of approximately 3.8 min, the detection wavelength was $\lambda = 254$ nm. The
 175 calibration curve was linear ($R > 0.999$) within the range of 0.06 to 0.00003 mg/mL. To
 176 determine the amount of dexamethasone potentially remaining in the implants after 35 d
 177 exposure to phosphate buffer pH 7.4, the remnants were freeze-dried for 3 d (Christ Epsilon 2–
 178 4 LSC; Martin Christ, Osterode, Germany) and the lyophilisates were dissolved in a mixture of
 179 acetonitrile and ethanol (2:1 v/v). The solutions were filtered using 0.45 μm PVDF filter
 180 syringes, and analyzed for their drug contents by HPLC-UV (as described above). In case of
 181 incomplete drug release at the end of the observation period, the “missing” amounts were
 182 experimentally recovered in the implant remnants. All experiments were conducted in triplicate.
 183 In addition, the pH of the release medium was measured at pre-determined time points using a
 184 pH meter (InoLab pH Level 1; WTW, Weilheim, Germany) ($n = 3$).

185 Implant swelling and erosion: At pre-determined time points, implant samples were
 186 withdrawn, excess water carefully removed using Kimtech precision wipes (Kimberly-Clark,
 187 Rouen, France) and weighed [*wet mass* (t)]. The samples were lyophilized for 3 d (Christ
 188 Epsilon 2–4 LSC) and weighed again [*dry mass* (t)]. The *wet mass* (%) (t), *water/NMP content*
 189 (%) (t), and *dry mass loss* (%) (t) were calculated as follows:

$$190$$

$$191 \quad \text{wet mass (\%)(}t\text{)} = \frac{\text{wet mass (}t\text{)}}{\text{formulation mass}} \times 100 \%$$

$$192 \quad (1)$$

$$193 \quad \text{water/NMP content (\%)(}t\text{)} = \frac{\text{wet mass (}t\text{)} - \text{dry mass (}t\text{)}}{\text{wet mass (}t\text{)}} \times 100 \%$$

$$194 \quad (2)$$

$$195 \quad \text{dry mass loss (\%)(}t\text{)} = \frac{\text{dry mass (0)} - \text{dry mass (}t\text{)}}{\text{dry mass (0)}} \times 100 \%$$

$$196 \quad (3)$$

197 where *formulation mass* is the initial total mass of the liquid formulation (PLGA +
198 dexamethasone + NMP), and *dry mass (0)* is the dry mass of the liquid formulation prior to
199 exposure to the release medium (PLGA + dexamethasone). All experiments were conducted in
200 triplicate.

201 Polymer degradation: At pre-determined time points, implants were withdrawn, freeze-
202 dried and the lyophilisates were dissolved in tetrahydrofuran (at a concentration of 3 mg/mL).
203 The average polymer molecular weight (Mw) of the PLGA was determined by Gel Permeation
204 Chromatography (GPC, Separation Modules e2695 and e2695D, 2419 RI Detector, Empower
205 GPC software; Waters, Guyancourt, France) using a PLGel 5 μ m MIXED-D column, 7.5 x
206 300 mm (Agilent Technologies, Interchim, Montluçon, France). The injection volume was
207 50 μ L. Tetrahydrofuran was the mobile phase (flow rate: 1 mL/min). Polystyrene standards
208 with molecular weights between 1,090 and 70,950 Da (Polymer Laboratories, Varian, Les Ulis,
209 France) were used to prepare the calibration curve. All experiments were conducted in
210 triplicate.

211 Implant morphology: At pre-determined time points, implants were withdrawn and
212 optionally freeze-dried. Cross-sections were obtained by manual breaking. Pictures were taken
213 with an optical image analysis system (Nikon SMZ-U; Nikon, Tokyo, Japan), equipped with a
214 Zeiss camera (AxioCam ICc1; Zeiss, Jena, Germany).

215

216 **2.5. Determination of the drug solubility**

217 The solubility of dexamethasone (as received) in phosphate buffer pH 7.4 at 37 °C was
218 determined in agitated glass flasks. An excess amount of dexamethasone powder
219 (approximately 30 mg) was exposed to 80 mL bulk fluid, kept at 37 °C under horizontal shaking
220 (80 rpm; GFL 3033). Samples were withdrawn, filtered (0.45 μ m PVDF syringe filter), diluted

221 and analyzed for their drug content by HPLC-UV (as described above, using an injection
222 volume of 20 μ L) until equilibrium was reached. Each experiment was conducted in triplicate.

223

224

225 **3. Results and Discussion**

226

227 **3.1. Importance of the volume of the release medium**

228 Since the investigated implants are formed *in-situ* following solvent exchange, it was
229 important to evaluate the impact of the volume of the release medium into which the
230 PLGA/drug/NMP solutions were injected. Potentially, the volume of this aqueous phase can
231 affect the diffusion rate of NMP into the surrounding aqueous phase and/or the diffusion rate
232 of water into the (initially) liquid formulation. Such changes might affect the resulting implant
233 size and inner structure and, hence, the drug release kinetics.

234 The volume of vitreous humor in humans has been reported to be about 4 to 5 mL (Bennett,
235 2016). To monitor potential effects of variations in the bulk fluid volume in this order of
236 magnitude on the key properties of the *in-situ* formed implants, 2.25 and 4.5 mL have been
237 investigated in this study. Furthermore, most drugs are eliminated via the anterior pathway
238 (Toris et al., 1999; Urtti, 2006). To simulate drug elimination and fluid renewal, the release
239 medium was completely exchanged every day during the first week (which is most decisive for
240 implant formation) in this study.

241 Figure 1 shows macroscopic pictures of PLGA-based implants formed upon injection of
242 100 μ L of a PLGA/dexamethasone/NMP solution into 2.25 or 4.5 mL phosphate buffer pH 7.4
243 (37 °C). The liquid formulations contained 30 % Resomer RG 502H and 0.75 %
244 dexamethasone. The photos were taken after 3 d. At the top, implants in Eppendorf tubes (filled
245 with the release medium) are shown. Below, higher magnifications of implants, which had been

246 carefully withdrawn from the release medium are illustrated (surfaces). At the bottom, surfaces
247 and cross-sections of implant samples after freeze-drying are shown. The cross-sections were
248 obtained by manual breaking. The dashed regions highlight the hollow cores of the implants.
249 As it can be seen, there was no remarkable impact of the volume of the aqueous bulk fluid (2.25
250 vs. 4.5 mL) on the resulting implant morphology: left vs. right hand side in Figure 1. Please
251 note that caution must be paid when drawing conclusions from the pictures of lyophilized
252 implants, because of artifact creation during freeze-drying. Importantly, the implants were
253 hollow also in the wet state (data not shown). This can be explained as follows: Upon contact
254 with water, NMP diffuses into the outer bulk fluid and water diffuses into the liquid NMP
255 formulation. Since PLGA is soluble in NMP, but not in water, at a certain time point the
256 polymer precipitates (once the solubility of the polymer in the water/NMP mixture is reached).
257 This process likely starts at the “formulation – aqueous bulk fluid” interface, because the water
258 concentration is highest and the NMP concentration lowest at this location. The continuous
259 decrease in PLGA solubility in the NMP/water mixture (the NMP content decreases, whereas
260 the water content increases) leads to continued polymer precipitation. Thus, the PLGA “shell”
261 becomes thicker and thicker, growing “inwards”. Once all PLGA has precipitated, potentially
262 remaining inner volumes (here the centers of the implants) cannot be filled with polymer and
263 become water-filled cavities. Please note that complete solvent exchange took up to several
264 days in this study: Thus, the implant cores remained liquid for a significant period of time.
265 Importantly, no noteworthy impact of the bulk fluid volume on this cavity formation was
266 observed.

267 Figures 2a and b show the resulting dexamethasone release kinetics and the dynamic
268 changes of the systems’ water/NMP contents over time. The water/NMP contents of the
269 implants were determined gravimetrically as the difference between the wet and dry mass of
270 the withdrawn samples (before and after freeze-drying). As it can be seen, the drug release

271 curves were virtually overlapping for the investigated bulk fluid volumes (2.25 vs. 4.5 mL).
272 Also, the resulting water/NMP contents were very similar. This can probably be attributed to
273 the fact that NMP and water are freely miscible: So, there are no saturation effects, resulting in
274 potentially reduced NMP diffusion rates into smaller (eventually more saturated) outer aqueous
275 phases (and vice versa).

276 Importantly, limited drug solubility effects in the surrounding release medium are unlikely
277 to affect dexamethasone release from the *in-situ* forming implants at an initial drug loading of
278 0.75 %: The solubility of dexamethasone in phosphate buffer pH 7.4 at 37 °C was determined
279 to be 77 ± 4 µg/mL. In NMP, the drug is freely soluble. Thus, at early time points (when the
280 surrounding bulk fluid contains considerable amounts of NMP) saturation effects in the
281 surrounding bulk fluid are unlikely. Furthermore, even if assuming the absence of any NMP in
282 the surrounding bulk fluid from day 3 on (this is a “worst case scenario” for the drug solubility),
283 sink conditions were also provided for the remaining observation period (considering the drug
284 solubility determined in pure phosphate buffer pH 7.4 at 37 °C).

285 These findings are important, since they demonstrate that variations in the volume of the
286 bulk fluid into which the PLGA/drug/NMP solutions are injected, are not substantially affecting
287 the key properties of the resulting implants. In other words: The proposed *in-situ* forming
288 implant formulations can be expected to be rather robust with respect to variations in the
289 vitreous humor volumes encountered *in vivo*.

290

291 **3.2. Impact of the drug loading**

292 Figure 3 shows the impact of the initial drug loading of the *in-situ* forming implant
293 formulations on the resulting dexamethasone release kinetics and the dynamic changes in the
294 implants' wet mass as well as water/NMP contents. The initial drug content was varied from
295 0.25 to 7.5 %, as indicated. Please note that 100 µL of the formulation with the intermediate

296 drug loading (0.75 %) contain a similar drug dose as the commercially available drug product
297 Ozurdex (0.7 mg) (Chan et al., 2011). The release medium was 2.25 mL phosphate buffer
298 pH 7.4. Resomer RG 502H (30 %) was the polymer. Clearly, the relative drug release rates
299 were similar for formulations loaded with 0.25 and 0.75 % dexamethasone (filled and open
300 circles in Figure 2a), whereas the relative drug release rate was substantially lower at 7.5 %
301 drug loading (filled triangles). This cannot be attributed to differences in the dynamic changes
302 in the systems' wet mass, as illustrated in Figure 3b (which were rather similar for all drug
303 loadings).

304 Given the limited solubility of dexamethasone in the release medium ($77 \pm 4 \mu\text{g/mL}$ in
305 phosphate buffer pH 7.4 at 37°C), one hypothesis can be that the substantially reduced drug
306 release rate at 7.5 % initial dexamethasone loading is due to saturation effects. To evaluate the
307 validity of this hypothesis, the renewal rate of the release medium was altered: Figures 4a and
308 b show the resulting drug release kinetics and degrees of bulk fluid saturation (with respect to
309 the drug) observed at a higher and lower sampling frequency (at each sampling time point, the
310 release medium was completely renewed). The degrees of saturation of the release medium
311 were calculated based on the solubility of dexamethasone in phosphate buffer pH 7.4 at 37°C .
312 Since the surrounding bulk fluid contained important amounts of NMP at early time points, and
313 since dexamethasone is soluble in NMP, no values are indicated in the first week (Figure 4b).
314 Clearly, the higher sampling frequency lead to faster drug release after about 1 week,
315 corresponding to lower degrees of bulk fluid saturation with the drug. Furthermore, after about
316 3 weeks, the degree of bulk fluid saturation substantially decreased (to about 10 % = sink
317 conditions) in the case of the higher sampling frequency, while the release rate *decreased*. These
318 observations indicate that saturation effects likely refer to both: dexamethasone saturation in
319 the *surrounding* bulk fluid as well as drug saturation effects *within* the implants: At an initial
320 drug loading of 7.5 %, important parts of the dexamethasone can be expected to precipitate

321 *within* the *in-situ* forming PLGA implants upon water penetration into and NMP leaching out
322 of the system. Consequently, dissolved and non-dissolved dexamethasone co-exist within the
323 implant. It has to be pointed out that only dissolved drug is available for diffusion and can be
324 released into the surrounding bulk fluid (Siepmann and Siepmann, 2012, 2008). Hence, drug
325 release is also likely to be limited by saturation effects *within* the implants.

326 Please note that during the first week, the observed dexamethasone release rates were very
327 similar for the lower and higher sampling frequency (filled and open circles in Figure 4a). This
328 might be explained by the fact that during this time period noteworthy amounts of NMP were
329 still present *within* the implants and the surrounding bulk fluid (limiting the importance of drug
330 saturation effects).

331 Furthermore, the initial drug loading had no major impact on the resulting dynamic changes
332 in the implants' wet mass over time (Figure 3b). The latter increased during the first 2.5 weeks,
333 and then decreased again. The initial increase can be attributed to the progressing PLGA
334 degradation and subsequent water penetration into the more and more hydrophilic polymer
335 matrices. The subsequent decrease is likely attributable to the dissolution/disappearance of the
336 remnants (more hydrated regions dissolving faster than less hydrated regions). The water/NMP
337 contents were very high during the observation period, irrespective of the initial drug loading
338 (Figure 3c).

339

340 **3.3. Impact of the PLGA polymer molecular weight**

341 The effects of the polymer molecular weight of the PLGA on drug release and the dynamic
342 changes in the implants' wet mass as well as water/NMP contents upon exposure to phosphate
343 buffer pH 7.4 are illustrated in Figure 5: Resomer RG 502H (Mw about 15 k Da) and Resomer
344 RG 504H (Mw about 45 k Da) are compared. The initial dexamethasone loading was 0.25 %,
345 the polymer concentration in the liquid formulation was 30 %, and the volume of the release

346 medium was 2.25 mL. As it can be seen, the polymer molecular weight substantially impacted
347 the dynamic changes in the systems' wet mass and water/NMP content: Implants based on
348 longer chain PLGA took up fundamentally less water than systems based on shorter chain
349 PLGA. This can be attributed to the facts that: (i) longer chain PLGA is more hydrophobic than
350 shorter chain PLGA, and (ii) longer chain PLGA is likely to precipitate earlier than shorter
351 chain PLGA upon water penetration into the system and NMP diffusion out of the formulation.
352 The observed differences in the wet mass of the implants based on shorter and longer chain
353 PLGA (Figure 5b) are consistent with the different water/NMP contents of systems (Figure 5c).
354 Whereas the implants based on the more hydrophilic Resomer RG 502H show high water
355 contents right from the beginning, the water contents of Resomer RG 504H-based systems was
356 initially substantially lower, but significantly increased during the observation period (due to
357 the progressive polymer chain cleavage). From a practical point of view, substantial implant
358 swelling should be avoided to minimize any related side effects in vivo. This might for instance
359 be achieved via the selection of appropriate PLGA molecular weights or monomer (lactic acid:
360 glycolic acid) ratios, or specific additives (Do et al., 2014, 2015a,b).

361 Interestingly, these substantial differences in the implants' compositions and water uptake
362 behaviors are "not fully" reflected in the observed release kinetics (Figure 5a). This is because
363 drug release was almost complete within the first few days: the time period of implant
364 formation. For instance, after 4 d only 3.8 ± 0.8 and 10.5 ± 1.0 % dexamethasone remained
365 trapped within the implants based on Resomer RG 502H and Resomer RG 504H, respectively.
366 These amounts were slowly released during the subsequent 3 weeks. The observed slower drug
367 release from Resomer RG 504H-based implants compared to Resomer RG 502H-based
368 implants can at least partially be attributed to the lower water contents of the systems (and, thus,
369 denser polymer networks). Please note that with other drugs, which are not almost completely
370 released within the first few days during implant formation, substantial differences in the

371 resulting release kinetics can be expected from Resomer RG 502H- and Resomer RG 504H-
372 based implants, due to the fundamentally different conditions for drug release in these systems
373 (Figures 5b and c).

374

375 **3.4. Impact of the polymer concentration**

376 Figure 6 shows the observed dexamethasone release kinetics from *in-situ* formed implants
377 prepared with drug-polymer solutions in NMP containing 30 vs. 45% Resomer RG 502H, or
378 15 vs. 30 % Resomer RG 504H. Please note that in the latter case, higher polymer
379 concentrations lead to considerable viscosities, rendering injection difficult. The volume of the
380 release medium was 2.25 mL, the initial drug content 0.25 %. As it can be seen, the polymer
381 concentration in the liquid formulations affected the resulting drug release kinetics, irrespective
382 of the PLGA polymer molecular weight: With increasing polymer concentration the
383 dexamethasone release rate decreased. This can at least partially be attributed to differences in
384 the implants' inner structure, as shown in Figure 7: At the top, cross-sections of freeze-dried
385 implants based on Resomer RG 502H are illustrated, at the bottom cross-sections of implants
386 based on Resomer RG 504H. The implants were lyophilized after 3 d exposure to phosphate
387 buffer pH 7.4. Again, please note that caution should be paid because of potential artifact
388 creation during freeze-drying. The dashed regions indicate the hollow central implant cavities.
389 Clearly, higher polymer concentrations in the liquid formulations lead to smaller cavities. This
390 can be attributed to the fact that PLGA precipitation started at the "liquid formulation – aqueous
391 bulk fluid" interface. Subsequent PLGA precipitation "filled" the *in-situ* forming implants. In
392 the case of higher polymer concentrations, more polymer was available to fill the interior of the
393 systems, resulting in smaller cavities. The thicker the polymer shells, the longer are the
394 diffusion pathways through the PLGA matrices to be overcome by the trapped drug. Thus,

395 higher polymer concentrations in the formulations lead to thicker polymer shells/barriers and,
396 hence, slower drug release (irrespective of the polymer molecular weight).

397 Furthermore, the smaller central implant cavities at higher initial PLGA concentrations
398 resulted in lower increases in the systems' wet mass and lower water contents, irrespective of
399 the PLGA polymer molecular weight (Figures 8 and 9). Figures 10 to 12 illustrate the dynamic
400 changes in the polymer molecular weight (Mw) of the PLGA, the pH of the surrounding bulk
401 fluid and the dry mass loss kinetics of the systems. Importantly, the smaller central implant
402 cavities observed at higher initial polymer concentrations lead to accelerated ester chain
403 cleavage (Figure 10: open symbols always below filled symbols). This can be attributed to an
404 increase in the importance of autocatalytic effects in these systems: Water is present throughout
405 the implants, thus, polymer chain cleavage occurs in the entire polymer matrices. The generated
406 (water-soluble) shorter chain acids slowly diffuse into the surrounding bulk fluid, where they
407 are (at least partially) neutralized. In addition, bases from the surrounding phosphate buffer
408 diffuse into the implants and neutralize (at least partially) the generated acids. However, the
409 rate at which the acids are generated within the implants can be higher than the rate at which
410 they are neutralized. Consequently, the micro-pH can locally drop (Brunner et al., 1999; Ding
411 and Schwendeman, 2004; Li and Schwendeman, 2005; Ding and Schwendeman, 2008;
412 Schädlich et al., 2014), resulting in pH gradients within the implants. Since hydrolytic ester
413 bond cleavage is catalyzed by protons, PLGA degradation is accelerated at locations with low
414 pH values (Grizzi et al., 1995; Lu et al., 1999). The importance of such autocatalytic effects
415 strongly depends on the systems' dimensions and porosity (Siepmann et al., 2005; Klose et al.,
416 2006). With increasing polymer concentration in the liquid formulation the thickness of the
417 polymer "shells" increases (Figure 7), hence, autocatalysis is likely more pronounced. The
418 experimentally measured PLGA degradation kinetics shown in Figure 10 clearly confirm this
419 hypothesis: The polymer backbone is more rapidly cleaved at higher PLGA concentrations

420 (open vs. filled symbols). Interestingly, this faster PLGA degradation at higher polymer
421 concentrations is not reflected in the drug release kinetics (Figure 6), demonstrating the
422 dominance of the thickness of the PLGA shells (the lengths of the diffusion pathways through
423 the polymeric matrices) in this case.

424 Furthermore, the diffusion of the short chain acids out of the implants into the surrounding
425 bulk fluid can lead to a decrease in pH of the latter. As it can be seen in Figure 11, decreasing
426 pH values of the release medium were indeed observed in all cases. At higher polymer
427 concentrations the “pH drops” were much more pronounced than in the case of lower PLGA
428 concentrations, irrespective of the polymer molecular weight. This can probably be attributed
429 to the fact that thicker polymer “shells” are created at high PLGA concentrations, resulting in
430 more pronounced autocatalytic effects (since the generated short chain acids more slowly
431 diffuse out and bases from the release medium more slowly diffuse in, due to the longer
432 diffusion pathways to be overcome). The potential consequences of (slight) acidifications of
433 the surrounding environment in vivo should be addressed in future studies. The fact that
434 dexamethasone is an anti-inflammatory drug might help minimizing tissue irritation, but
435 caution should be taken when speculating on these aspects based on in vitro data.

436 Comparing the dynamic changes in the pH values of the surrounding bulk fluids in the case
437 of implants based on Resomer RG 502H and Resomer RG 504H (Figure 11 a vs. 11b), it can
438 be seen that the “pH drops” occur at later time points in the case of the longer chain PLGA.
439 This can at least partially be attributed to the fact that the initial polymer molecular weight was
440 higher, thus, more time is needed to generate short chain, water-soluble acids, which can diffuse
441 out. Interestingly, the “*clear* pH drops” in the bulk fluid observed at higher polymer
442 concentrations (open symbols in Figures 11a,b) are followed by distinct increases in the
443 systems’ dry mass loss (open symbols in Figures 12a,b): The dry mass loss nicely reflects the
444 leaching of the shorter chain (water-soluble) acids out of the implants into the release medium.

445 **4. Conclusion**

446 *In-situ* forming PLGA-based implants offer an interesting potential for ocular
447 dexamethasone delivery. Importantly, the systems can be expected to be rather robust with
448 respect to variations in the vitreous humor volumes encountered *in vivo*. Depending on the
449 initial drug loading, drug saturation effects *within* the implants and in the surrounding aqueous
450 medium can play an important role for the control of dexamethasone release. The polymer
451 molecular weight as well as the PLGA concentration in the liquid formulations determine *how*
452 the macromolecules precipitate as well as the extent and rate of system swelling. These are key
453 features, being decisive for the mobility of water, drug, polymer degradation products and bases
454 within the system. For example, they affect the thickness of the polymer shell, water content of
455 the system and importance of local drops in the micro-pH (and, thus, autocatalysis). The inner
456 implant structure and conditions for mass transport within the *in-situ* forming implants
457 determine polymer degradation and drug release.

458 In the future, the toxicity of the solvent NMP for the ocular tissue as well as the potential
459 consequences of local drops in pH due to leaching of PLGA degradation products should be
460 studied *in vivo*. It would also be interesting to investigate the effects of the monomer ratio
461 (lactic acid to glycolic acid) of the PLGA as well as the impact of potential additives, altering
462 the formation of the implants and the conditions for mass transport. Such formulation changes
463 might be used to adjust desired release kinetics for given drugs and drug doses during specific
464 target release periods.

465

466 **References**

- 467 Agossa, K., Lizambard, M., Rongthong, T., Delcourt-Debruyne, E., Siepmann, J., Siepmann,
468 F., 2017. Physical key properties of antibiotic-free, PLGA/HPMC-based in-situ forming
469 implants for local periodontitis treatment. *Int. J. Pharm.* 521, 282–293.
470 <https://doi.org/10.1016/j.ijpharm.2017.02.039>
- 471 Bennett, L., 2016. Other Advances in Ocular Drug Delivery, in: Addo, R.T. (Ed.), *Ocular Drug*
472 *Delivery: Advances, Challenges and Applications*. Springer International Publishing,
473 pp. 165–185. https://doi.org/10.1007/978-3-319-47691-9_10
- 474 Bisht, R., Jaiswal, J.K., Oliver, V.F., Eurtivong, C., Reynisson, J., Rupenthal, I.D., 2017.
475 Preparation and evaluation of PLGA nanoparticle-loaded biodegradable light-
476 responsive injectable implants as a promising platform for intravitreal drug delivery. *J.*
477 *Drug Deliv. Sci. Technol.* 40, 142–156. <https://doi.org/10.1016/j.jddst.2017.06.006>
- 478 Bonilha, V.L., Shadrach, K.G., Rayborn, M.E., Li, Y., Pauer, G.J.T., Hagstrom, S.A.,
479 Bhattacharya, S.K., Hollyfield, J.G., 2013. Retinal deimination and PAD2 levels in
480 retinas from donors with age-related macular degeneration (AMD). *Exp. Eye Res.* 111,
481 71–78. <https://doi.org/10.1016/j.exer.2013.03.017>
- 482 Brunner, A., Mäder, K., Göpferich, A., 1999. pH and Osmotic Pressure Inside Biodegradable
483 Microspheres During Erosion1. *Pharm. Res.* 16, 847–853.
484 <https://doi.org/10.1023/A:1018822002353>
- 485 Chan, A., Leung, L.-S., Blumenkranz, M.S., 2011. Critical appraisal of the clinical utility of the
486 dexamethasone intravitreal implant (Ozurdex®) for the treatment of macular edema
487 related to branch retinal vein occlusion or central retinal vein occlusion. *Clin.*
488 *Ophthalmol. Auckl. NZ* 5, 1043–1049. <https://doi.org/10.2147/OPHTH.S13775>
- 489 Chiou, G.C.Y., 2011. Pharmacological treatment of dry age-related macular degeneration
490 (AMD). *Taiwan J. Ophthalmol.* 1, 2–5. <https://doi.org/10.1016/j.tjo.2011.08.001>

- 491 Desai, K.G.H., Mallery, S.R., Schwendeman, S.P., 2008. Effect of formulation parameters on
492 2-methoxyestradiol release from injectable cylindrical poly(dl-lactide-co-glycolide)
493 implants. *Eur. J. Pharm. Biopharm.* 70, 187–198.
494 <https://doi.org/10.1016/j.ejpb.2008.03.007>
- 495 Ding, A.G., Schwendeman, S.P., 2008. Acidic Microclimate pH Distribution in PLGA
496 Microspheres Monitored by Confocal Laser Scanning Microscopy. *Pharm. Res.* 25,
497 2041–2052. <https://doi.org/10.1007/s11095-008-9594-3>
- 498 Ding, A.G., Schwendeman, S.P., 2004. Determination of water-soluble acid distribution in
499 poly(lactide-co-glycolide). *J. Pharm. Sci.* 93, 322–331.
500 <https://doi.org/10.1002/jps.10524>
- 501 Do, M.P., Neut, C., Delcourt, E., Seixas Certo, T., Siepmann, J., Siepmann, F., 2014. In situ
502 forming implants for periodontitis treatment with improved adhesive properties. *Eur. J.*
503 *Pharm. Biopharm.* 88, 342–350. <https://doi.org/10.1016/j.ejpb.2014.05.006>
- 504 Do, M.P., Neut, C., Metz, H., Delcourt, E., Mäder, K., Siepmann, J., Siepmann, F., 2015a. In-
505 situ forming composite implants for periodontitis treatment: How the formulation
506 determines system performance. *Int. J. Pharm.* 486, 38–51.
507 <https://doi.org/10.1016/j.ijpharm.2015.03.026>
- 508 Do, M.P., Neut, C., Metz, H., Delcourt, E., Siepmann, J., Mäder, K., Siepmann, F., 2015b.
509 Mechanistic analysis of PLGA/HPMC-based in-situ forming implants for periodontitis
510 treatment. *Eur. J. Pharm. Biopharm.* 94, 273–283.
511 <https://doi.org/10.1016/j.ejpb.2015.05.018>
- 512 Droege, K.M., Muether, P.S., Hermann, M.M., Caramoy, A., Viebahn, U., Kirchhof, B., Fauser,
513 S., 2013. Adherence to ranibizumab treatment for neovascular age-related macular
514 degeneration in real life. *Graefes Arch. Clin. Exp. Ophthalmol.* 251, 1281–1284.
515 <https://doi.org/10.1007/s00417-012-2177-3>

- 516 Edelhauser, H.F., Rowe-Rendleman, C.L., Robinson, M.R., Dawson, D.G., Chader, G.J.,
517 Grossniklaus, H.E., Rittenhouse, K.D., Wilson, C.G., Weber, D.A., Kuppermann, B.D.,
518 Csaky, K.G., Olsen, T.W., Kompella, U.B., Holers, V.M., Hageman, G.S., Gilger, B.C.,
519 Campochiaro, P.A., Whitcup, S.M., Wong, W.T., 2010. Ophthalmic Drug Delivery
520 Systems for the Treatment of Retinal Diseases: Basic Research to Clinical Applications.
521 *Investig. Ophthalmology Vis. Sci.* 51, 5403. <https://doi.org/10.1167/iovs.10-5392>
- 522 Fredenberg, S., Wahlgren, M., Reslow, M., Axelsson, A., 2011. The mechanisms of drug
523 release in poly(lactic-co-glycolic acid)-based drug delivery systems—A review. *Int. J.*
524 *Pharm.* 415, 34–52. <https://doi.org/10.1016/j.ijpharm.2011.05.049>
- 525 Gasmi, H., Danede, F., Siepmann, J., Siepmann, F., 2015a. Does PLGA microparticle swelling
526 control drug release? New insight based on single particle swelling studies. *J. Controlled*
527 *Release* 213, 120–127. <https://doi.org/10.1016/j.jconrel.2015.06.039>
- 528 Gasmi, H., Siepmann, F., Hamoudi, M.C., Danede, F., Verin, J., Willart, J.-F., Siepmann, J.,
529 2016. Towards a better understanding of the different release phases from PLGA
530 microparticles: Dexamethasone-loaded systems. *Int. J. Pharm.*, In Honour of Professor
531 Alexander T. Florence In Honour of Professor Alexander T. Florence 514, 189–199.
532 <https://doi.org/10.1016/j.ijpharm.2016.08.032>
- 533 Gasmi, H., Willart, J.-F., Danede, F., Hamoudi, M.C., Siepmann, J., Siepmann, F., 2015b.
534 Importance of PLGA microparticle swelling for the control of prilocaine release. *J. Drug*
535 *Deliv. Sci. Technol.* 30, 123–132. <https://doi.org/10.1016/j.jddst.2015.10.009>
- 536 Ghalanbor, Z., Körber, M., Bodmeier, R., 2013. Interdependency of protein-release
537 completeness and polymer degradation in PLGA-based implants. *Eur. J. Pharm.*
538 *Biopharm.* 85, 624–630. <https://doi.org/10.1016/j.ejpb.2013.03.031>

- 539 Ghazala, F., Hovan, M., Mahmood, S., 2013. Improving treatment provision of Wet AMD with
540 intravitreal ranibizumab. *BMJ Qual. Improv. Rep.* 2, u201733.w993.
541 <https://doi.org/10.1136/bmjquality.u201733.w993>
- 542 Giudice, G.L., Galan, A., 2012. Basic Research and Clinical Application of Drug Delivery
543 Systems for the Treatment of Age-Related Macular Degeneration.
544 <https://doi.org/10.5772/31524>
- 545 Grizzi, I., Garreau, H., Li, S., Vert, M., 1995. Hydrolytic degradation of devices based on
546 poly(dl-lactic acid) size-dependence. *Biomaterials* 16, 305–311.
547 [https://doi.org/10.1016/0142-9612\(95\)93258-F](https://doi.org/10.1016/0142-9612(95)93258-F)
- 548 Hamoudi-Ben Yelles, M.C., Tran Tan, V., Danede, F., Willart, J.F., Siepmann, J., 2017. PLGA
549 implants: How Poloxamer/PEO addition slows down or accelerates polymer
550 degradation and drug release. *J. Controlled Release* 253, 19–29.
551 <https://doi.org/10.1016/j.jconrel.2017.03.009>
- 552 Hirota, K., Doty, A.C., Ackermann, R., Zhou, J., Olsen, K.F., Feng, M.R., Wang, Y., Choi, S.,
553 Qu, W., Schwendeman, A.S., Schwendeman, S.P., 2016. Characterizing release
554 mechanisms of leuprolide acetate-loaded PLGA microspheres for IVIVC development
555 I: In vitro evaluation. *J. Controlled Release*, The 14th edition of the European
556 Symposium on Controlled Drug Delivery, Egmond aan Zee, The Netherlands on April
557 13-15, 2016 244, 302–313. <https://doi.org/10.1016/j.jconrel.2016.08.023>
- 558 Huang, J., Mazzara, J.M., Schwendeman, S.P., Thouless, M.D., 2015. Self-healing of pores in
559 PLGAs. *J. Controlled Release* 206, 20–29.
560 <https://doi.org/10.1016/j.jconrel.2015.02.025>
- 561 Hughes, P.M., Olejnik, O., Chang-Lin, J.-E., Wilson, C.G., 2005. Topical and systemic drug
562 delivery to the posterior segments. *Adv. Drug Deliv. Rev.*, Drug Delivery Strategies to

- 563 Treat Age-Related Macular Degeneration 57, 2010–2032.
564 <https://doi.org/10.1016/j.addr.2005.09.004>
- 565 Kaur, I.P., Kakkar, S., 2014. Nanotherapy for posterior eye diseases. *J. Controlled Release* 193,
566 100–112. <https://doi.org/10.1016/j.jconrel.2014.05.031>
- 567 Kempe, S., Mäder, K., 2012. In situ forming implants — an attractive formulation principle for
568 parenteral depot formulations. *J. Controlled Release, Drug Delivery Research in Europe*
569 161, 668–679. <https://doi.org/10.1016/j.jconrel.2012.04.016>
- 570 Kempe, S., Metz, H., Pereira, P.G.C., Mäder, K., 2010. Non-invasive in vivo evaluation of in
571 situ forming PLGA implants by benchtop magnetic resonance imaging (BT-MRI) and
572 EPR spectroscopy. *Eur. J. Pharm. Biopharm., Imaging Techniques in Drug*
573 *Development* 74, 102–108. <https://doi.org/10.1016/j.ejpb.2009.06.008>
- 574 Klose, D., Siepmann, F., Elkharraz, K., Krenzlin, S., Siepmann, J., 2006. How porosity and size
575 affect the drug release mechanisms from PLGA-based microparticles. *Int. J. Pharm.,*
576 *Local Controlled Drug Delivery to the Brain* 314, 198–206.
577 <https://doi.org/10.1016/j.ijpharm.2005.07.031>
- 578 Kowluru, R.A., Mishra, M., 2015. Oxidative stress, mitochondrial damage and diabetic
579 retinopathy. *Biochim. Biophys. Acta BBA - Mol. Basis Dis.* 1852, 2474–2483.
580 <https://doi.org/10.1016/j.bbadis.2015.08.001>
- 581 Kranz, H., Bodmeier, R., 2008. Structure formation and characterization of injectable drug
582 loaded biodegradable devices: In situ implants versus in situ microparticles. *Eur. J.*
583 *Pharm. Sci.* 34, 164–172. <https://doi.org/10.1016/j.ejps.2008.03.004>
- 584 Kranz, H., Bodmeier, R., 2007. A novel in situ forming drug delivery system for controlled
585 parenteral drug delivery. *Int. J. Pharm.* 332, 107–114.
586 <https://doi.org/10.1016/j.ijpharm.2006.09.033>

- 587 Kranz, H., Ubrich, N., Maincent, P., Bodmeier, R., 2000. Physicomechanical Properties of
588 Biodegradable Poly(D,L-lactide) and Poly(D,L-lactide-co-glycolide) Films in the Dry
589 and Wet States. *J. Pharm. Sci.* 89, 1558–1566. [https://doi.org/10.1002/1520-
590 6017\(200012\)89:12<1558::AID-JPS6>3.0.CO;2-8](https://doi.org/10.1002/1520-6017(200012)89:12<1558::AID-JPS6>3.0.CO;2-8)
- 591 Kurz, P.A., Suhler, E.B., Flaxel, C.J., Rosenbaum, J.T., 2008. Injectable Intraocular
592 Corticosteroids, in: Becker, M., Davis, J. (Eds.), *Surgical Management of Inflammatory
593 Eye Disease*. Springer Berlin Heidelberg, pp. 5–16. [https://doi.org/10.1007/978-3-540-
594 33862-8_1](https://doi.org/10.1007/978-3-540-33862-8_1)
- 595 Li, L., Schwendeman, S.P., 2005. Mapping neutral microclimate pH in PLGA microspheres. *J.
596 Controlled Release, Proceedings of the Eight European Symposium on Controlled Drug
597 Delivery* 101, 163–173. <https://doi.org/10.1016/j.jconrel.2004.07.029>
- 598 Lu, L., Garcia, C.A., Mikos, A.G., 1999. In vitro degradation of thin poly(DL-lactic-co-glycolic
599 acid) films. *J. Biomed. Mater. Res.* 46, 236–244.
- 600 Luan, X., Skupin, M., Siepmann, J., Bodmeier, R., 2006. Key parameters affecting the initial
601 release (burst) and encapsulation efficiency of peptide-containing poly(lactide-co-
602 glycolide) microparticles. *Int. J. Pharm.* 324, 168–175.
603 <https://doi.org/10.1016/j.ijpharm.2006.06.004>
- 604 Parent, M., Clarot, I., Gibot, S., Derive, M., Maincent, P., Leroy, P., Boudier, A., 2017. One-
605 week in vivo sustained release of a peptide formulated into in situ forming implants. *Int.
606 J. Pharm.* 521, 357–360. <https://doi.org/10.1016/j.ijpharm.2017.02.046>
- 607 Parent, M., Nouvel, C., Koerber, M., Sapin, A., Maincent, P., Boudier, A., 2013. PLGA in situ
608 implants formed by phase inversion: Critical physicochemical parameters to modulate
609 drug release. *J. Controlled Release* 172, 292–304.
610 <https://doi.org/10.1016/j.jconrel.2013.08.024>

- 611 Rodrigues, E.B., Grumann, A., Penha, F.M., Shiroma, H., Rossi, E., Meyer, C.H., Stefano, V.,
612 Maia, M., Magalhaes, O., Farah, M.E., 2011. Effect of needle type and injection
613 technique on pain level and vitreal reflux in intravitreal injection. *J. Ocul. Pharmacol.*
614 *Ther. Off. J. Assoc. Ocul. Pharmacol. Ther.* 27, 197–203.
615 <https://doi.org/10.1089/jop.2010.0082>
- 616 Rodríguez Villanueva, J., Rodríguez Villanueva, L., Guzmán Navarro, M., 2017.
617 Pharmaceutical technology can turn a traditional drug, dexamethasone into a first-line
618 ocular medicine. A global perspective and future trends. *Int. J. Pharm.* 516, 342–351.
619 <https://doi.org/10.1016/j.ijpharm.2016.11.053>
- 620 Schädlich, A., Kempe, S., Mäder, K., 2014. Non-invasive in vivo characterization of
621 microclimate pH inside in situ forming PLGA implants using multispectral fluorescence
622 imaging. *J. Controlled Release* 179, 52–62.
623 <https://doi.org/10.1016/j.jconrel.2014.01.024>
- 624 Schoenhammer, K., Boisclair, J., Schuetz, H., Petersen, H., Goepferich, A., 2010.
625 Biocompatibility of an injectable in situ forming depot for peptide delivery. *J. Pharm.*
626 *Sci.* 99, 4390–4399. <https://doi.org/10.1002/jps.22149>
- 627 Schoenhammer, K., Petersen, H., Guethlein, F., Goepferich, A., 2009. Injectable in situ forming
628 depot systems: PEG-DAE as novel solvent for improved PLGA storage stability. *Int. J.*
629 *Pharm.* 371, 33–39. <https://doi.org/10.1016/j.ijpharm.2008.12.019>
- 630 Schwendeman, S.P., Shah, R.B., Bailey, B.A., Schwendeman, A.S., 2014. Injectable controlled
631 release depots for large molecules. *J. Controlled Release*, 30th Anniversary Special
632 Issue 190, 240–253. <https://doi.org/10.1016/j.jconrel.2014.05.057>
- 633 Siepman, J., Elkharraz, K., Siepman, F., Klose, D., 2005. How Autocatalysis Accelerates
634 Drug Release from PLGA-Based Microparticles: A Quantitative Treatment.
635 *Biomacromolecules* 6, 2312–2319. <https://doi.org/10.1021/bm050228k>

- 636 Siepmann, J., Siepmann, F., 2012. Modeling of diffusion controlled drug delivery. *J. Controlled*
637 *Release, Drug Delivery Research in Europe* 161, 351–362.
638 <https://doi.org/10.1016/j.jconrel.2011.10.006>
- 639 Siepmann, J., Siepmann, F., 2008. Mathematical modeling of drug delivery. *Int. J. Pharm.,*
640 *Future Perspectives in Pharmaceutics Contributions from Younger Scientists* 364, 328–
641 343. <https://doi.org/10.1016/j.ijpharm.2008.09.004>
- 642 Thakur, R.R.S., McMillan, H.L., Jones, D.S., 2014. Solvent induced phase inversion-based in
643 situ forming controlled release drug delivery implants. *J. Controlled Release* 176, 8–23.
644 <https://doi.org/10.1016/j.jconrel.2013.12.020>
- 645 Toris, C.B., Yablonski, M.E., Wang, Y.-L., Camras, C.B., 1999. Aqueous humor dynamics in
646 the aging human eye. *Am. J. Ophthalmol.* 127, 407–412. [https://doi.org/10.1016/S0002-](https://doi.org/10.1016/S0002-9394(98)00436-X)
647 [9394\(98\)00436-X](https://doi.org/10.1016/S0002-9394(98)00436-X)
- 648 Ueda, H., Hacker, M. c., Haesslein, A., Jo, S., Ammon, D. m., Borazjani, R. n., Kunzler, J. f.,
649 Salamone, J. c., Mikos, A. g., 2007. Injectable, in situ forming poly(propylene
650 fumarate)-based ocular drug delivery systems. *J. Biomed. Mater. Res. A* 83A, 656–666.
651 <https://doi.org/10.1002/jbm.a.31226>
- 652 Urtti, A., 2006. Challenges and obstacles of ocular pharmacokinetics and drug delivery. *Adv.*
653 *Drug Deliv. Rev., Ocular Drug Delivery* 58, 1131–1135.
654 <https://doi.org/10.1016/j.addr.2006.07.027>
- 655 Wan, T.-T., Li, X.-F., Sun, Y.-M., Li, Y.-B., Su, Y., 2015. Recent advances in understanding
656 the biochemical and molecular mechanism of diabetic retinopathy. *Biomed.*
657 *Pharmacother.* 74, 145–147. <https://doi.org/10.1016/j.biopha.2015.08.002>
- 658 Wilson, C.G., Tan, L.E., Mains, J., 2011. Principles of Retinal Drug Delivery from Within the
659 Vitreous, in: Kompella, U.B., Edelhauser, H.F. (Eds.), *Drug Product Development for*

660 the Back of the Eye, AAPS Advances in the Pharmaceutical Sciences Series. Springer
661 US, pp. 125–158.

662 Wykoff, C.C., Croft, D.E., Brown, D.M., Wang, R., Payne, J.F., Clark, L., Abdelfattah, N.S.,
663 Sadda, S.R., 2015. Prospective Trial of Treat-and-Extend versus Monthly Dosing for
664 Neovascular Age-Related Macular Degeneration: TREX-AMD 1-Year Results.
665 Ophthalmology 122, 2514–2522. <https://doi.org/10.1016/j.ophtha.2015.08.009>

666 Yasin, M.N., Svirskis, D., Seyfoddin, A., Rupenthal, I.D., 2014. Implants for drug delivery to
667 the posterior segment of the eye: A focus on stimuli-responsive and tunable release
668 systems. J. Controlled Release 196, 208–221.
669 <https://doi.org/10.1016/j.jconrel.2014.09.030>

670 Ying, L., Tahara, K., Takeuchi, H., 2013. Drug delivery to the ocular posterior segment using
671 lipid emulsion via eye drop administration: Effect of emulsion formulations and surface
672 modification. Int. J. Pharm. 453, 329–335.
673 <https://doi.org/10.1016/j.ijpharm.2013.06.024>

674 Zaki, W.M.D.W., Zulkifley, M.A., Hussain, A., Halim, W.H.W.A., Mustafa, N.B.A., Ting,
675 L.S., 2016. Diabetic retinopathy assessment: Towards an automated system. Biomed.
676 Signal Process. Control 24, 72–82. <https://doi.org/10.1016/j.bspc.2015.09.011>

677

678 **Web references**

679 <http://eligard.com>, accessed on 30 June 2018

680 <https://iluvien.com>, accessed on January 30 2018

681 <https://www.merck-animal-health-usa.com/product/cattle/Nuflor-Injectable-Solution/1>,
682 accessed on 30 June 2018

683 <http://www.retisert.com>, accessed on January 30 2018

684 <https://www.zoetisus.com/products/dogs/doxirobe-gel.aspx>, accessed on 30 June 2018

Figure legends

686

687 Fig. 1. Macroscopic pictures of implants formed *in-situ* upon exposure to phosphate buffer
688 pH 7.4 before and after freeze drying (surfaces and cross-sections). The formulations
689 contained 0.75 % dexamethasone and 30 % PLGA 502H. The volume of the release
690 medium was 2.25 mL (left column) or 4.5 mL (right column). The pictures were taken
691 after 3 d. The dashed regions highlight the hollow cores of the implants.

692 Fig 2. Impact of the volume of the release medium (phosphate buffer pH 7.4) on: a) drug
693 release, and b) the dynamic changes in the water/NMP content of *in-situ* forming
694 implants. The formulations contained 0.75 % dexamethasone and 30 % PLGA 502H.
695 Mean values +/- standard deviation are indicated (n=3).

696 Fig. 3. Impact of the initial drug loading (indicated in the diagrams) of *in-situ* forming
697 implants on the resulting: a) drug release kinetics, b) dynamic changes in the wet mass
698 and c) dynamic changes in the water/NMP content of the systems after exposure to
699 phosphate buffer pH 7.4. The formulations contained 30 % PLGA 502H. The volume
700 of the release medium was 2.25 mL. Mean values +/- standard deviation are indicated
701 (n=3).

702 Fig. 4. Impact of the sampling frequency during the drug release measurements on: a) the
703 cumulative relative amount of drug released, and b) the degree of saturation of the
704 withdrawn samples. The formulations contained 7.5 % dexamethasone and 30 %
705 PLGA 502H. The volume of the release medium was 4.5 mL. Mean values +/-
706 standard deviation are indicated (n=3).

707 Fig. 5. Importance of the polymer molecular weight of the PLGA (Resomer 502H vs. 504H)
708 for: a) drug release, b) the dynamic changes in the wet mass, and c) the dynamic
709 changes in the water/NMP content from/of implants formed *in-situ* upon exposure to
710 phosphate buffer pH 7.4. The formulations contained 0.25 % dexamethasone and

711 30 % PLGA. The volume of the release medium was 2.25 mL. Mean values +/-
712 standard deviation are indicated (n=3).

713 Fig. 6. Impact of the PLGA concentration in the formulation on the resulting dexamethasone
714 release kinetics from *in-situ* formed implants upon exposure to 2.25 mL phosphate
715 buffer pH 7.4: a) PLGA 502H and b) PLGA 504H. The drug content was 0.25 %.
716 Mean values +/- standard deviation are indicated (n=3).

717 Fig. 7. Macroscopic pictures of cross-sections of freeze-dried *in-situ* formed implants after
718 3 d exposure to 2.25 mL phosphate buffer 7.4. The formulations contained 0.25 %
719 dexamethasone and 30 % or 45 % PLGA 502H or 15 % or 30 % PLGA 504H. The
720 cross-sections were obtained by manual breaking. All implants were hollow, the
721 cavities are highlighted by the dashed areas.

722 Fig. 8. Impact of the PLGA concentration in the formulation on the dynamic changes in the
723 wet mass of implants formed *in-situ* upon exposure to 2.25 mL phosphate buffer
724 pH 7.4: a) PLGA 502H and b) PLGA 504H. The formulations contained 0.25 %
725 dexamethasone. Mean values +/- standard deviation are indicated (n=3).

726 Fig. 9. Effects of the PLGA concentration in the formulation on the dynamic changes in the
727 water/NMP content of implants formed *in-situ* upon exposure to 2.25 mL phosphate
728 buffer pH 7.4: a) PLGA 502H and b) PLGA 504H. The formulations contained
729 0.25 % dexamethasone. Mean values +/- standard deviation are indicated (n=3).

730 Fig. 10. Impact of the PLGA concentration in the formulation on PLGA degradation in
731 implants formed *in-situ* upon exposure to 2.25 mL phosphate buffer pH 7.4: a) PLGA
732 502H and b) PLGA 504H. The formulations contained 0.25 % dexamethasone. Mean
733 values +/- standard deviation are indicated (n=3).

734 Fig. 11. Effects of the PLGA concentration in the formulation on the dynamic changes in the
735 pH of the release medium surrounding implants formed *in-situ* upon exposure to

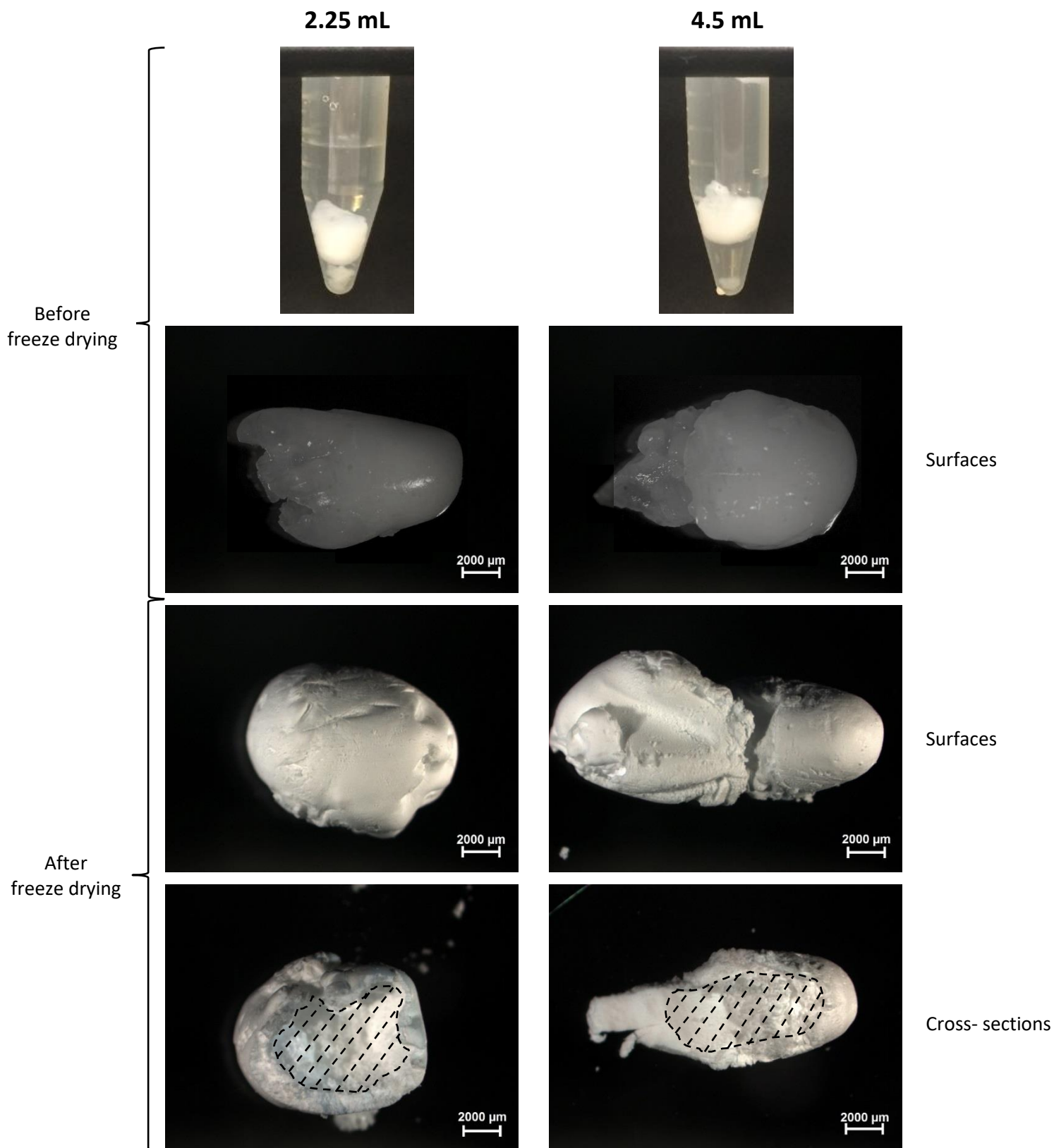
736 2.25 mL phosphate buffer pH 7.4: a) PLGA 502H and b) PLGA 504H. The
737 formulations contained 0.25 % dexamethasone. Mean values +/- standard deviation
738 are indicated (n=3).

739 Fig. 12. Impact of the PLGA concentration in the formulation on the dry mass loss of implants
740 formed *in-situ* upon exposure to 2.25 mL phosphate buffer pH 7.4: a) PLGA 502H
741 and b) PLGA 504H. The formulations contained 0.25 % dexamethasone. Mean values
742 +/- standard deviation are indicated (n=3).

743

744

745



746

747

Figure 1

748
749
750
751
752
753
754
755
756
757
758
759
760
761
762
763
764
765
766
767
768
769
770
771
772
773
774
775
776
777
778
779

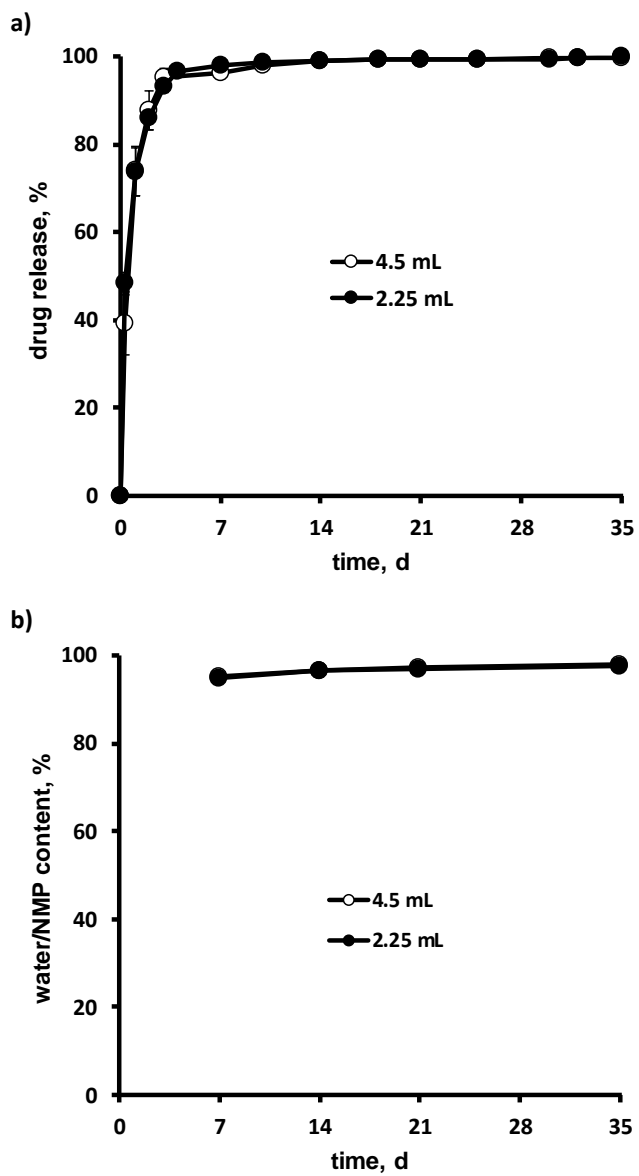


Figure 2

780
781
782
783
784
785
786
787
788
789
790
791
792
793
794
795
796
797
798
799
800
801
802
803
804
805
806
807
808
809
810
811
812
813
814
815

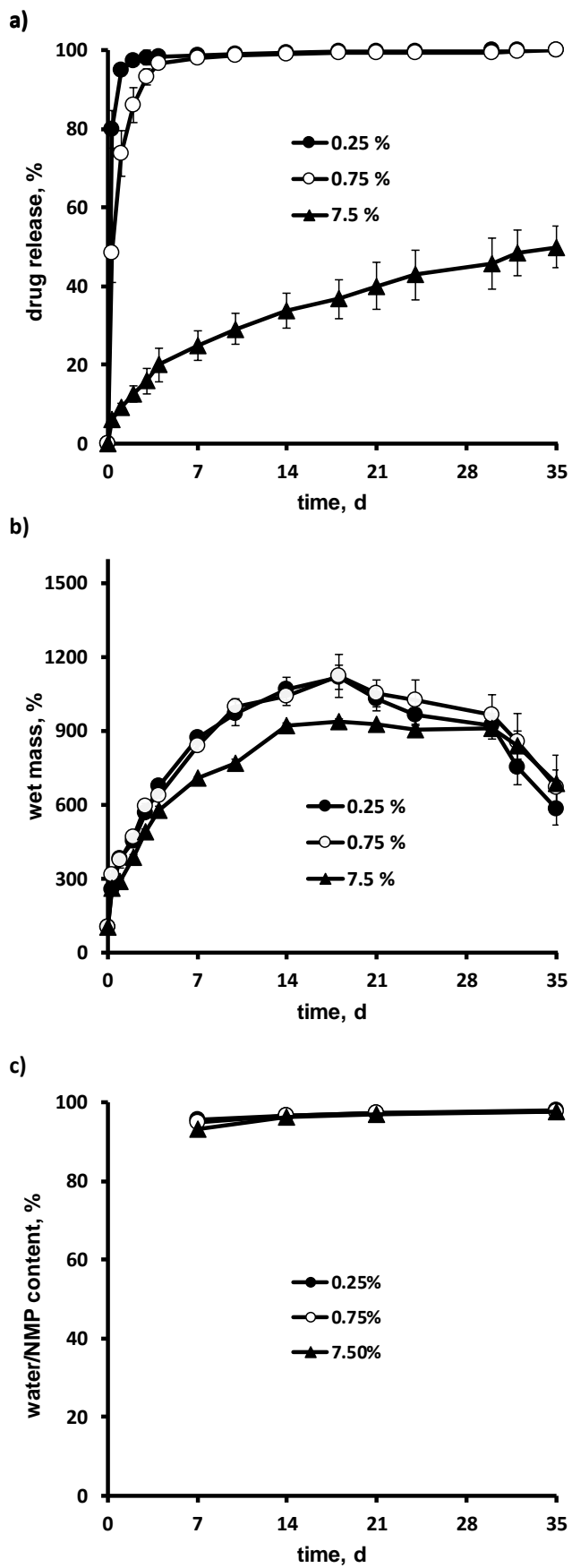


Figure 3

816
817
818
819
820
821
822
823
824
825
826
827
828
829
830
831
832
833
834
835
836
837
838
839
840
841
842
843
844
845
846
847
848

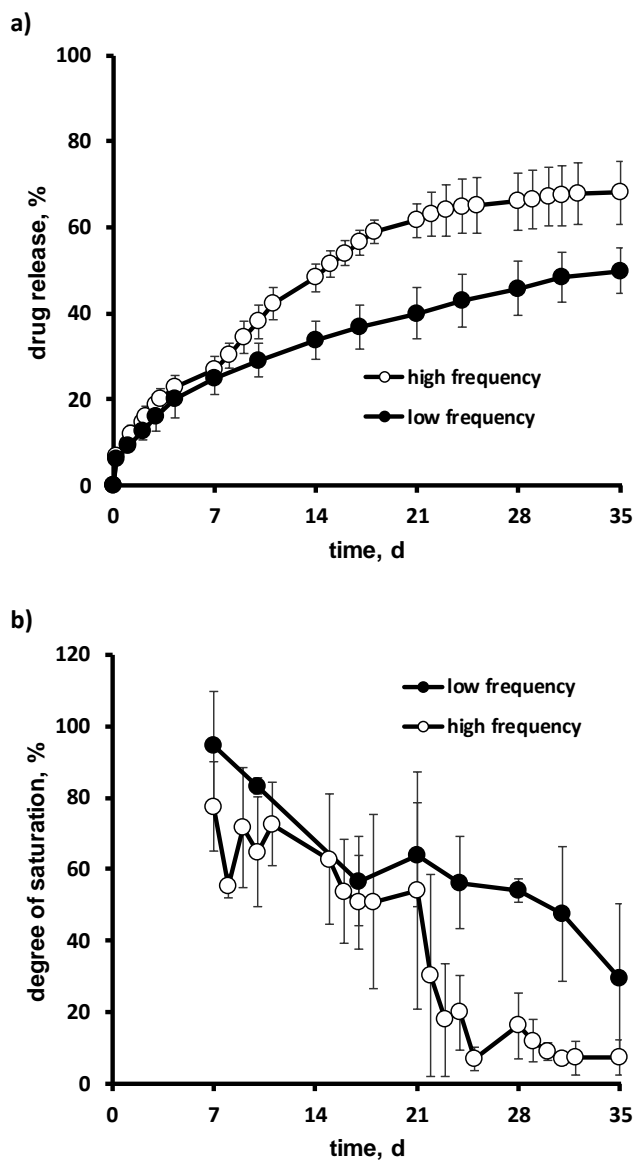


Figure 4

849
850
851
852
853
854
855
856
857
858
859
860
861
862
863
864
865
866
867
868
869
870
871
872
873
874
875
876
877
878
879
880
881
882
883
884

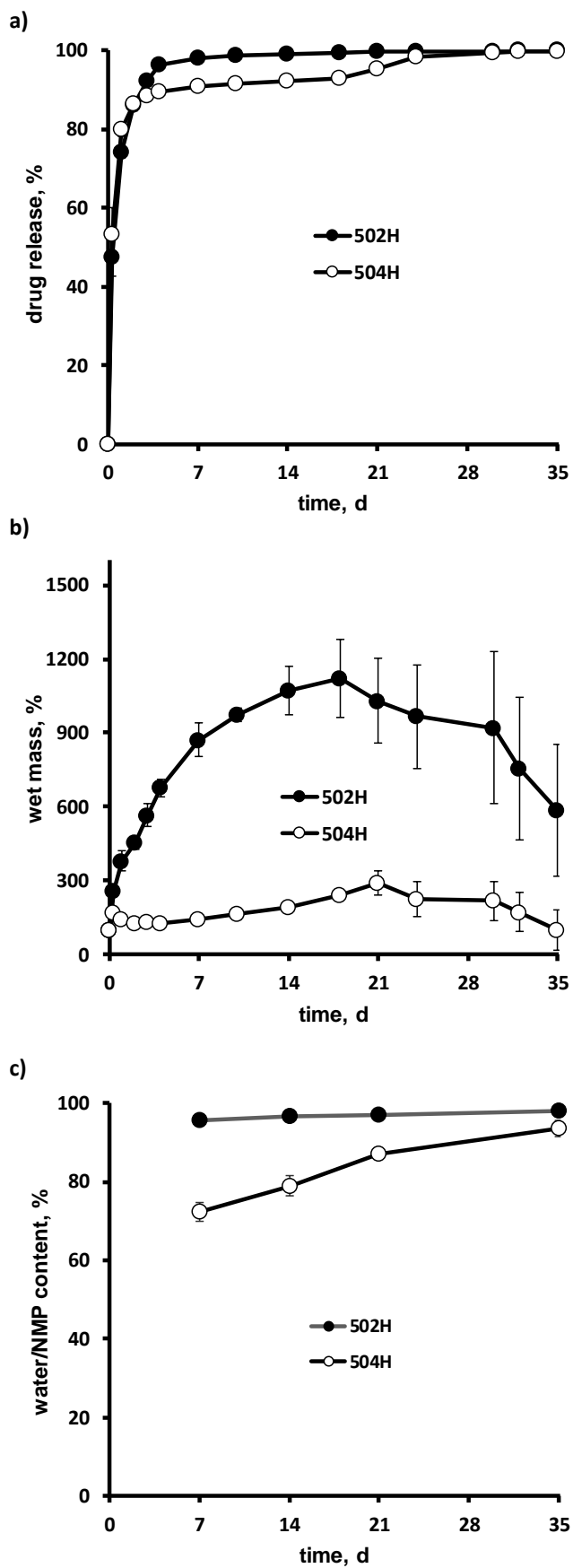


Figure 5

885
886
887
888
889
890
891
892
893
894
895
896
897
898
899
900
901
902
903
904
905
906
907
908
909
910
911
912
913
914
915
916

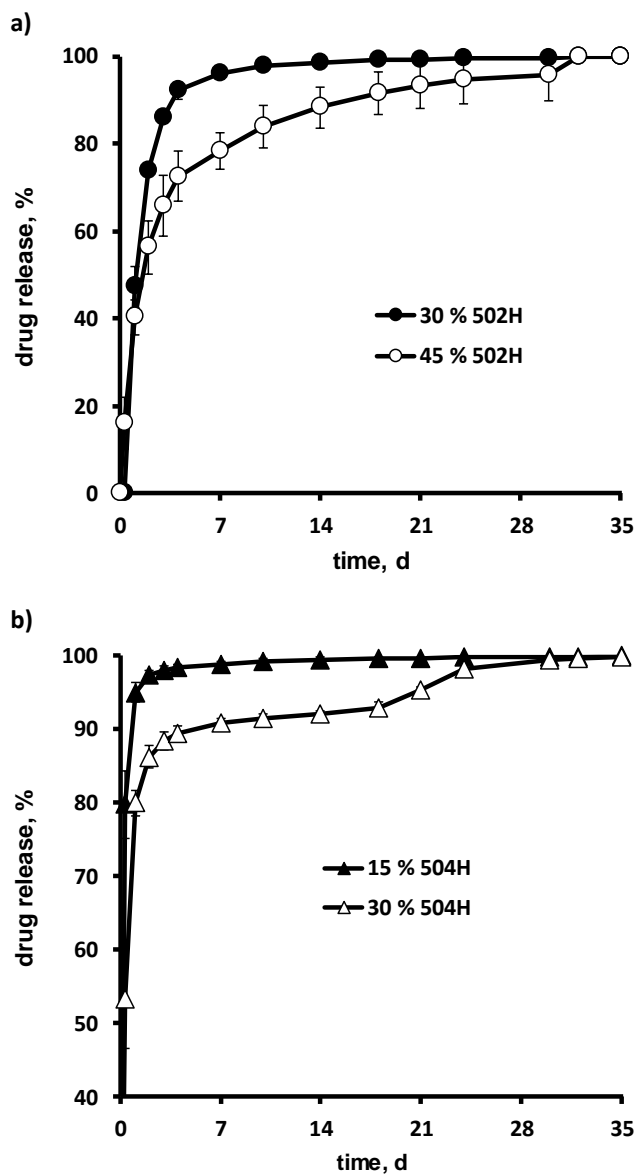
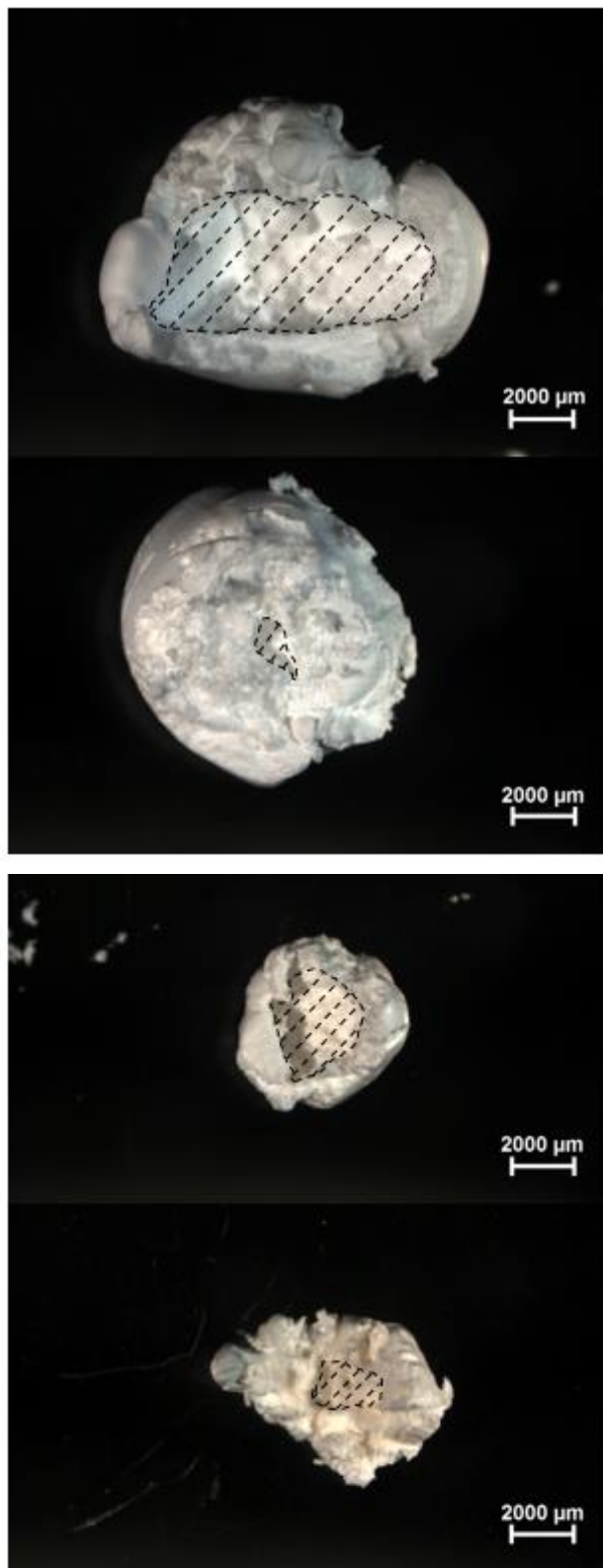


Figure 6



30 % 502H

45 % 502H

15 % 504H

30 % 504H

917

918

919

Figure 7

920
921
922
923
924
925
926
927
928
929
930
931
932
933
934
935
936
937
938
939
940
941
942
943
944
945
946
947
948
949
950
951
952
953
954
955

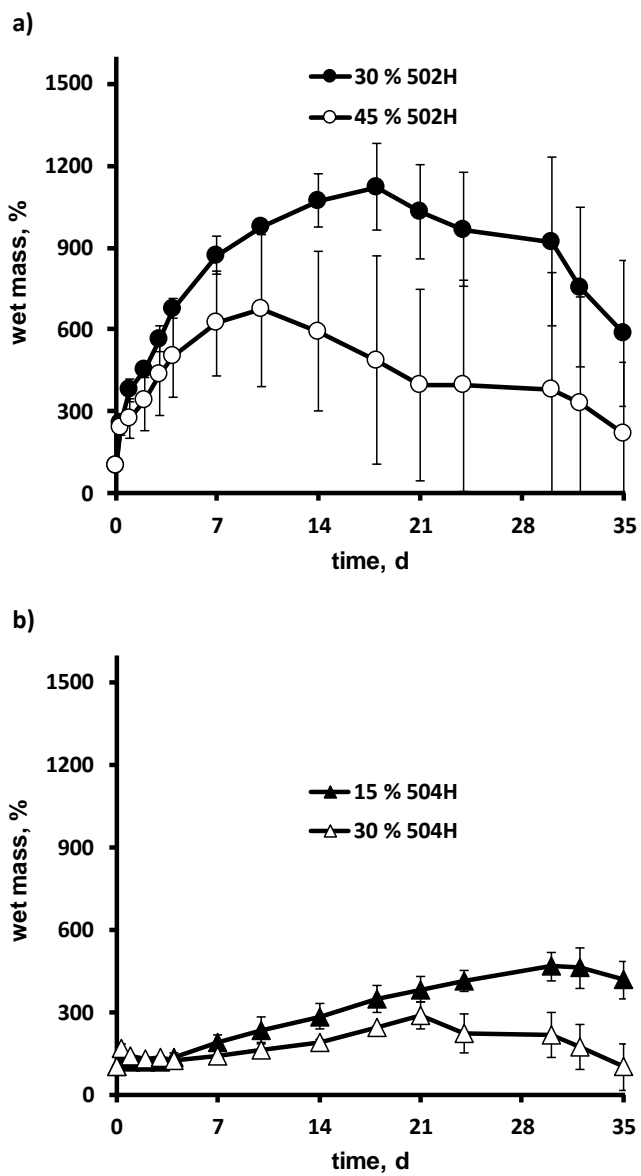


Figure 8

956
957
958
959
960
961
962
963
964
965
966
967
968
969
970
971
972
973
974
975
976
977
978
979
980
981
982
983
984
985
986
987
988
989

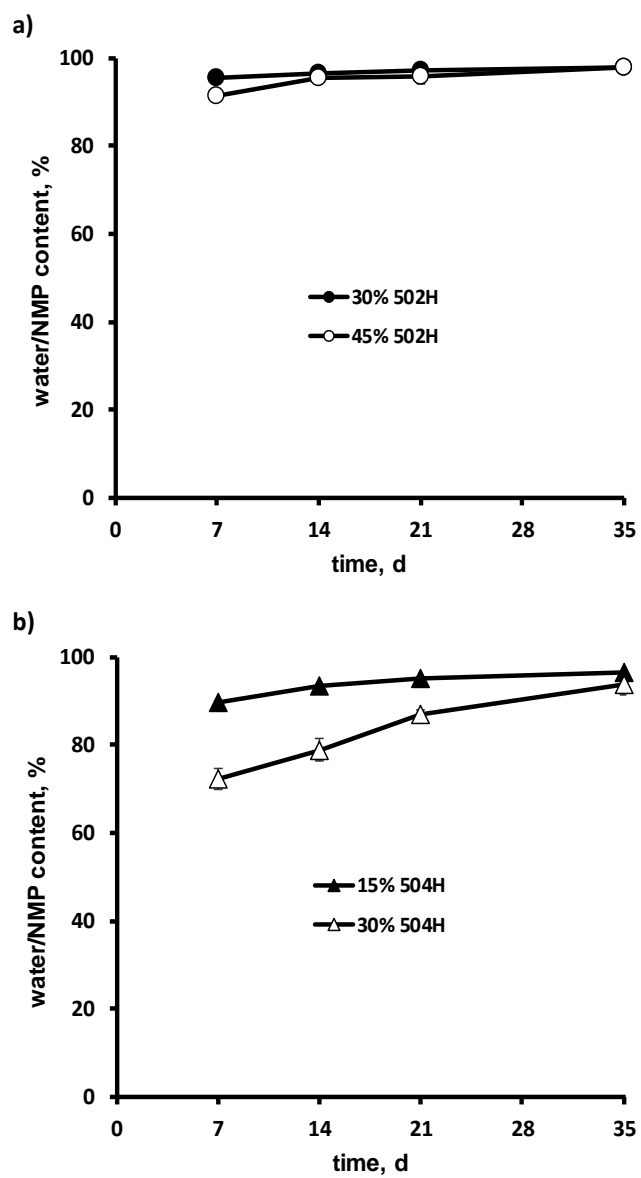


Figure 9

990
991
992
993
994
995
996
997
998
999
1000
1001
1002
1003
1004
1005
1006
1007
1008
1009
1010
1011
1012
1013
1014
1015
1016
1017
1018
1019
1020
1021

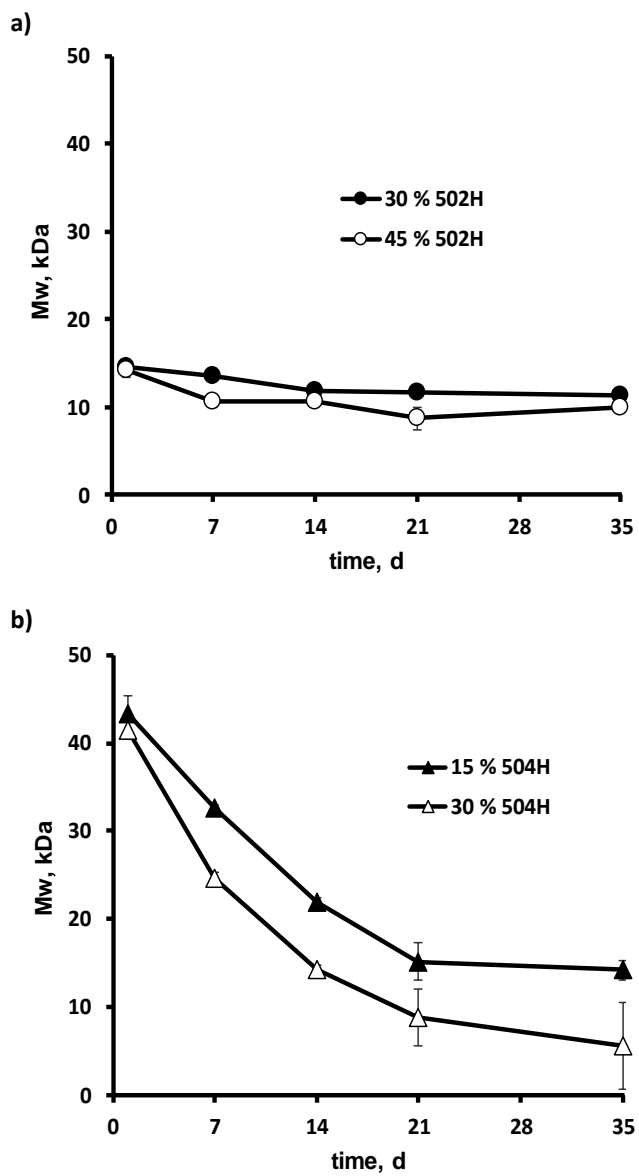


Figure 10

1022
1023
1024
1025
1026
1027
1028
1029
1030
1031
1032
1033
1034
1035
1036
1037
1038
1039
1040
1041
1042
1043
1044
1045
1046
1047
1048
1049
1050
1051
1052
1053
1054
1055

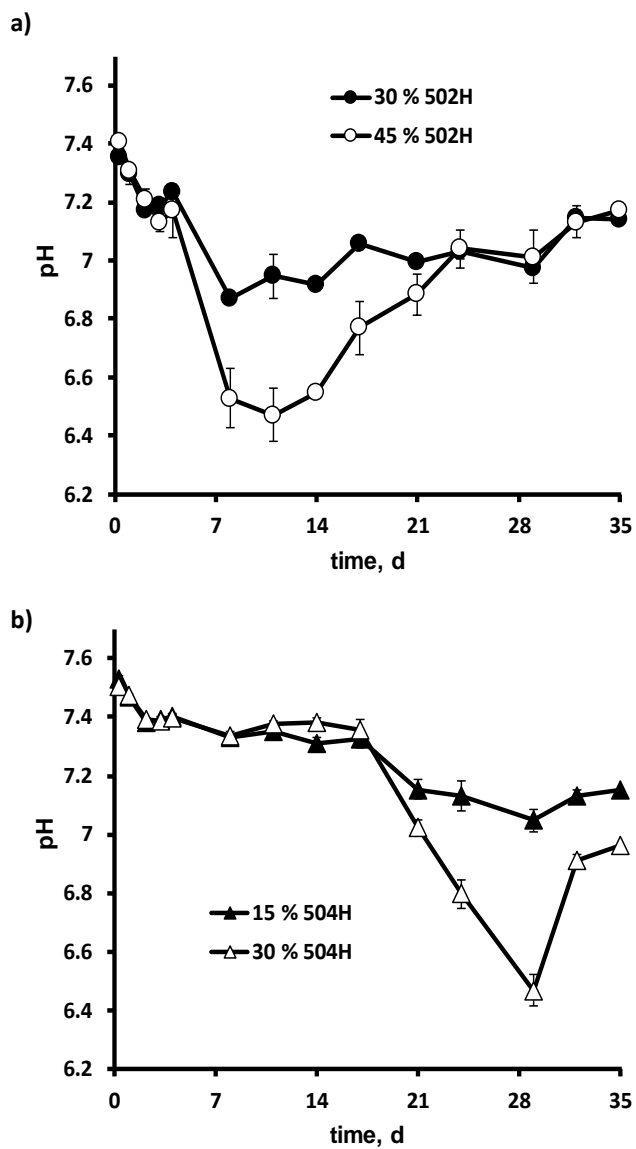


Figure 11

1056
1057
1058
1059
1060
1061
1062
1063
1064
1065
1066
1067
1068
1069
1070
1071
1072
1073
1074
1075
1076
1077
1078
1079
1080
1081
1082
1083
1084
1085
1086
1087

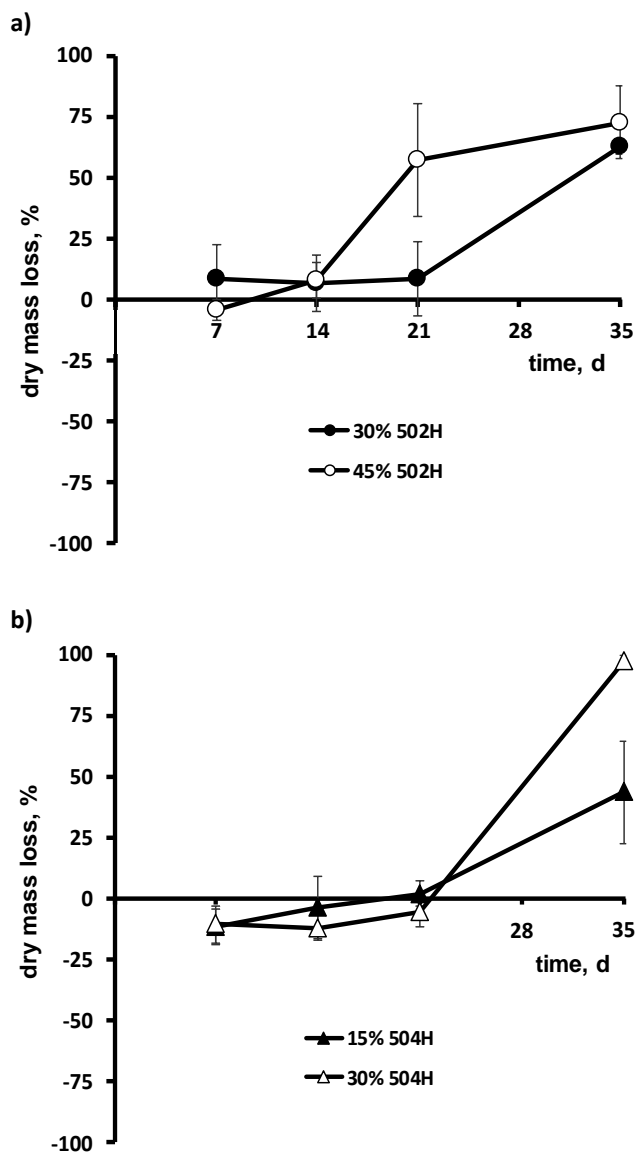


Figure 12